XVIII International Conference on Water Resources
CMWR 2010
J. Carrera (Ed)
CIMNE, Barcelona 2010

QUANTIFYING AND REDUCING HYDROGEOLOGIC UNCERTAINTY IN A FULLY-COUPLED LAND-ATMOSPHERE MODEL

John L. Williams, III and Reed M. Maxwell

Colorado School of Mines, Department of Geology and Geological Engineering, Hydrologic Science and Engineering Program, 1516 Illinois St., Golden, Colorado, USA

Key words: Land-atmosphere interactions, subsurface heterogeneity, fully-coupled models

Abstract. *Using ParFlow-WRF, a fully-coupled land-atmosphere model incorporating a variably saturated subsurface flow model, we evaluate responses in land-atmosphere feedbacks to heterogeneity in subsurface properties. To accomplish this, we first generate an idealized domain with heterogeneous, subsurface properties using correlated, Gaussian random fields. We then induce heavy rainfall using a moisture tendency over a straight line in the center of a fifteen by fifteen kilometer model grid within the atmospheric portion of the fully-coupled PF.WRF model grid domain to create changes in subsurface moisture and overland flow. We complete ensembles of model runs, each with different random seeds, and monitor the of surface runoff, saturation, and land-atmosphere feedbacks at and near the ground surface. Finally, using conditional Monte Carlo simulations, we also incorporate subsurface data to evaluate the reduction of uncertainty in soil moisture and subsequent impacts on land-atmosphere feedbacks.*

1 INTRODUCTION

Analyses and predictions involving the subsurface are challenging because it is not possible to develop a complete picture of subsurface heterogeneity with field data. Uncertainties associated with a heterogeneous subsurface can be reduced simply by adding more field data, but the cost of a dataset increases with each new data point. It then becomes important to carefully quantify if and how much data are needed to reduce uncertainty in the distribution of subsurface properties and the propagation of this uncertainty throughout the hydrologic cycle. Here, we use a fully-coupled subsurface-land surface-atmosphere model to evaluate responses in land-atmosphere feedbacks to varying heterogeneity in hydraulic conductivity in the subsurface to identify and reduce uncertainty in model predictions.

2 MODEL DOMAIN

The land-surface/subsurface (ParFlow) and atmospheric (WRF) portions of the PF.WRF model domain are set up separately. Horizontal discretization is the same for both, a 15 by 15 kilometer grid with 1000-meter resolution.

2.1 ParFlow domain

The ParFlow domain was constructed with a vertical resolution of 0.5 meters, a thickness

of 5 meters, and a 0.001 slope toward the west. The heterogeneous subsurface was produced using the turning bands algorithm[1]. The stochastic random field was constructed based on a mean hydraulic conductivity value of 0.01 m/s, horizontal correlation length of 5,000 meters, and vertical correlation length of 2 meters.

The boundary conditions for the ParFlow domain were set such that water enters the system only via rainfall, and leaves the system only via overland flow or evapotranspiration. This is accomplished using a Neumann-type (no flow) boundary condition for the lateral and bottom boundaries, and an overland flow boundary condition[2] for the land surface. Fluxes at and across the land surface are passed back and forth between ParFlow and the atmospheric portion of the model. The land surface and subsurface are forced by the coupled atmospheric model.

2.2 WRF domain

The atmospheric portion of the domain is discretized in terms of 25 transient pressure levels defined fractionally from the land surface to the top of the atmosphere at 14,960 Pa. This corresponds to a nominal vertical resolution of approximately 200 m near the surface and 800 m near the top of the atmosphere, which is at approximately 13,800 meters above mean sea level.

Periodic lateral boundary conditions[3] were imposed in all directions surrounding the domain. The upper boundary is the top of the atmosphere. The atmosphere is forced using idealized summer meteorological data, and precipitation induced by introducing antecedent moisture over pressure levels 8 through 17 (from the surface) across a straight north to south line in the center of the atmospheric domain during the first half of the 48-hour simulation.

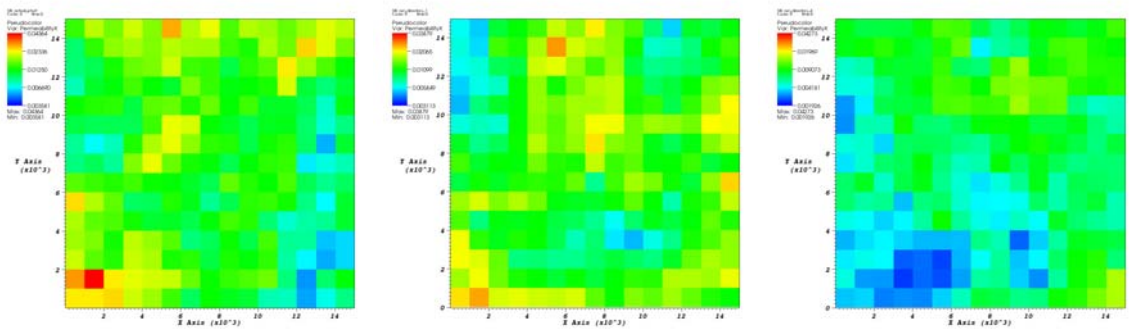

Figure 1: Hydraulic conductivity random fields were produced using the turning bands random field generator. Actual conditions are represented by the field at left.

3 COMPUTATIONAL APPROACH

ParFlow is a three-dimensional variably-saturated watershed model that simulates both subsurface and surface flow using an overland flow boundary condition[2,4,5]. It has been coupled to the Weather Research and Forcasting model (WRF)[3] passing fluxes through the land surface model Noah[6] resulting in a complete model of the hydrologic cycle[7].

We used ParFlow-WRF (PF.WRF) to run a ten-realization Monte Carlo simulation with

varying yet statistically equivalent subsurface heterogeneity. We also ran one additional simulation, the output of which represents the "actual" conditions of the hypothetical basin. We introduced antecedent moisture into the atmospheric domain and monitored the response at the land surface in terms of latent heat flux, saturation and wind velocity, and compared the results of the realizations with the "actual" conditions. The hydraulic conductivity fields for the actual basin and two example realizations are shown in Figure 1.

By generating random hydraulic conductivity fields over multiple realizations, each with a different random seed, we show a strong effect by varying subsurface heterogeneity on saturation, latent heat flux and wind speeds. This indicates that uncertainty in the subsurface will propagate through land-atmosphere feedbacks, and could have a profound effect on wind predictions used for applications such as wind energy forecasts.

In order to reduce the uncertainty of the heterogeneous subsurface, we seek to condition the hydraulic conductivity random field with data points from the actual hypothetical basin to form a narrow statistical envelope that captures the actual behavior exhibited in latent heat flux, saturation and wind speed within a 95 percent confidence interval.

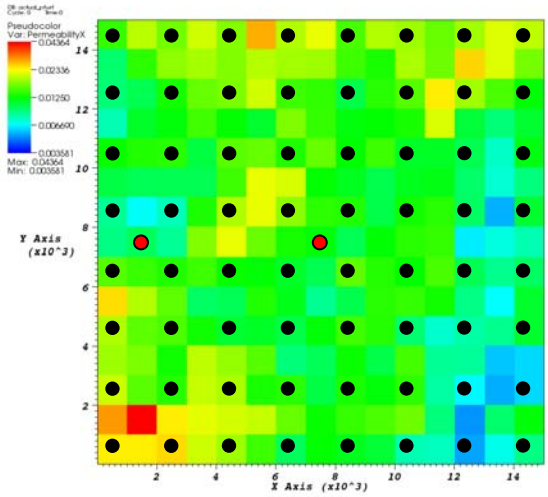

Figure 2: Observation points are shown in red—Point 1 at left, Point 7 at center—and conditioning points in black.

4 RESULTS AND DISCUSSION

We ran Monte Carlo simulations using hydraulic conductivity random fields without conditioning, with 18 conditioning points, 75 conditioning points, 144 conditioning points and 320 conditioning points. For this paper, we will discuss the cases without conditioning and with 320 conditioning points, shown on Figure 2. For our comparisons, we will look at two locations in the hypothetical basin, also shown on Figure 2—x = 1000 m, y = 7000 m, Point 1 near the edge of the domain, at the leading end of the runoff route, and away from the location of maximum rainfall, and x = 7000 m, y = 7000 m, Point 7 in the middle of the domain and in the area of maximum rainfall. The origin in this coordinate system is the southwest corner. We will concentrate on the second 24-hour period in the simulation, the recession period after

the moisture tendency has been removed.

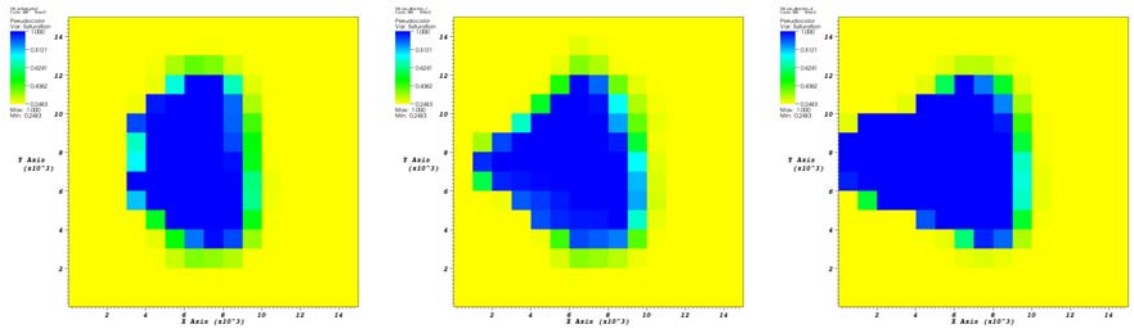

Figure 3: Surface saturation immediately following 24 hours of rainfall. Actual conditions shown on the left.

4.1 Unconditional Simulations

Figure 3 shows the variation in surface saturation and runoff routing between the actual conditions and two realizations at the end of the simulated rainstorm for the unconditional case. These plots are representative of the type of variation exhibited between realizations in the unconditional Monte Carlo simulation. Figure 4 shows the ensemble average saturation for the 10 realizations in the unconditional Monte Carlo simulation plotted with its 95 percent confidence interval envelope and the actual saturation at Point 1and Point 7. The ensemble average saturation increases during the rain period with a wide envelope encompassing saturations between 0 and 1. Point 7 becomes fully saturated during the simulation for all ten realizations, and the envelope is much smaller than at Point 1 during the recession period because all ten realizations begin the recession with nearly the same saturation value.

Figure 5 shows the actual and unconditional ensemble average latent heat flux with 95 percent confidence envelope at Point 1 and Point 7 during the recession period. Latent heat flux exhibits behavior similar to saturation. The 95 percent confidence envelope for latent heat flux at Point 1 is also wide. Latent heat flux at Point 7, like saturation, exhibits a narrower envelope than at Point 1.

Vertical wind speed exhibits more variation through time than saturation and latent heat flux, resulting in a noisy signal, as shown in Figure 6. The unconditional ensemble average appears to capture the diurnal cycle with higher wind speeds and a higher variance in wind speed during the day.

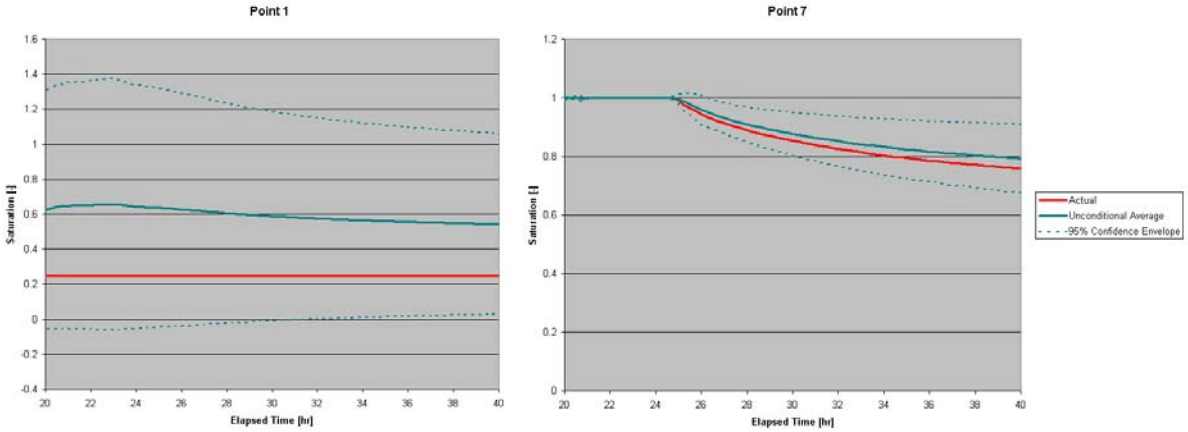

Figure 4: Unconditional average and actual saturation at Point 1 and Point 7 during the recession period are shown with the unconditional 95% confidence interval.

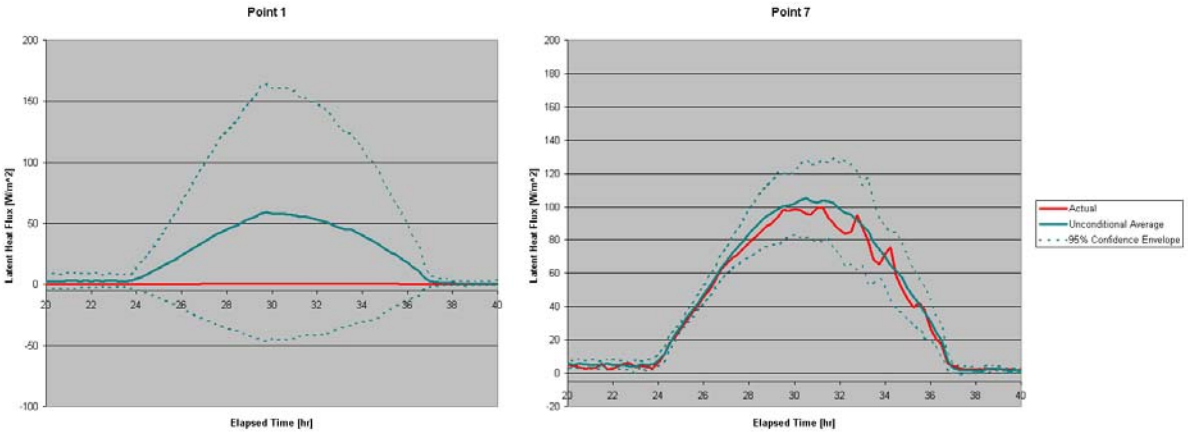

Figure 5: Unconditional average and actual latent heat flux at Point 1 and Point 7 during the recession period are shown with the unconditional 95% confidence interval.

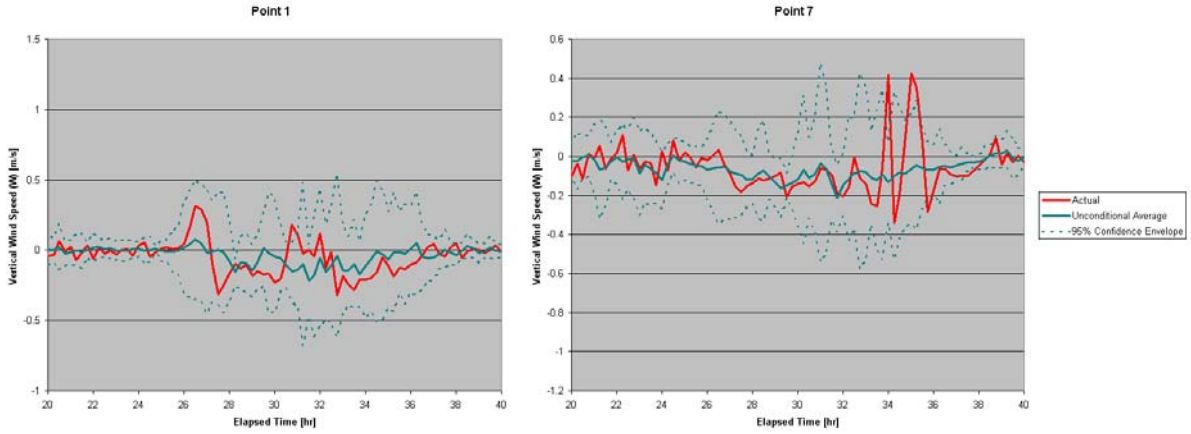

Figure 6: Unconditional average and actual vertical wind speed (W) at Point 1 and Point 7 during the recession period are shown with the unconditional 95% confidence interval.

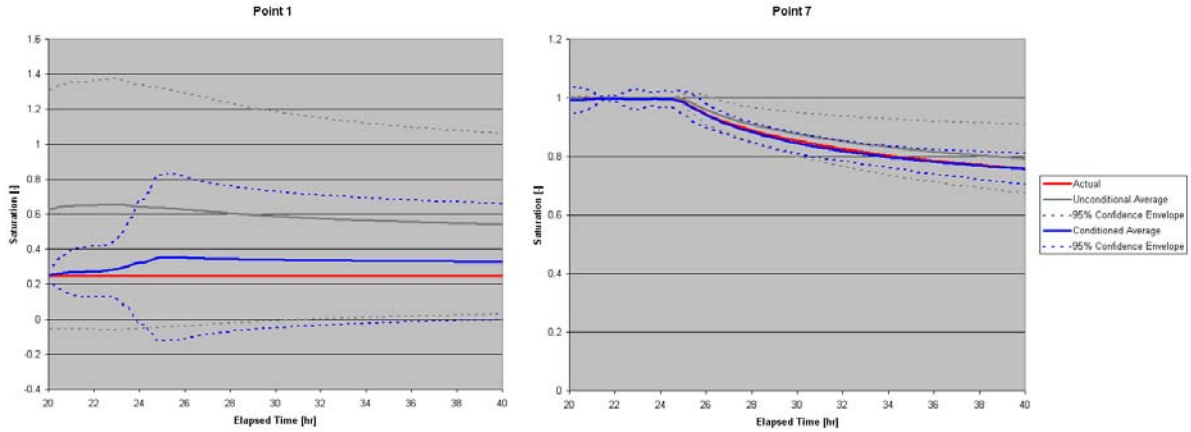

Figure 7: Conditioned average and actual saturation at Point 1 and Point 7 during the recession period are shown with the conditioned 95% confidence interval. Unconditional average and envelope are also shown.

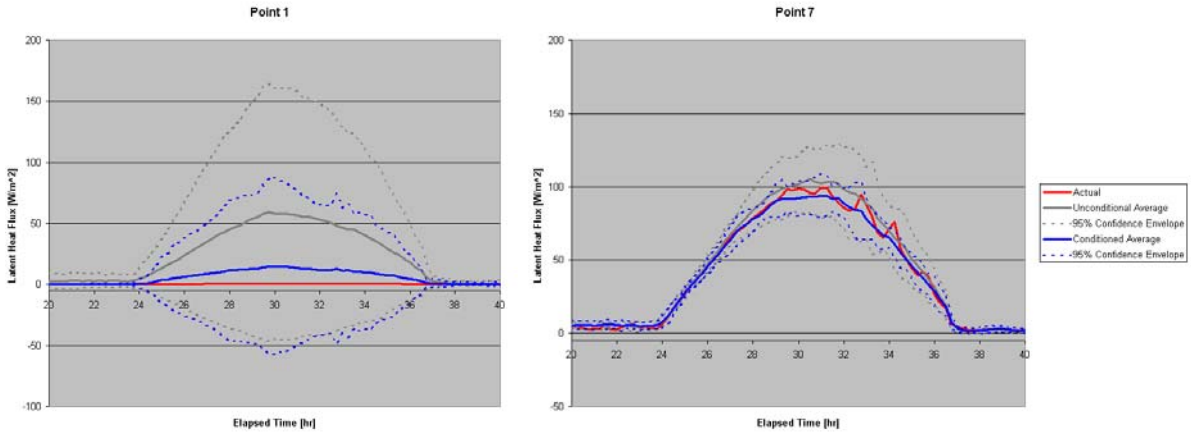

Figure 8: Conditioned average and actual latent heat flux at Point 1 and Point 7 during the recession period are shown with the conditioned 95% confidence interval. Unconditional average and envelope are also shown.

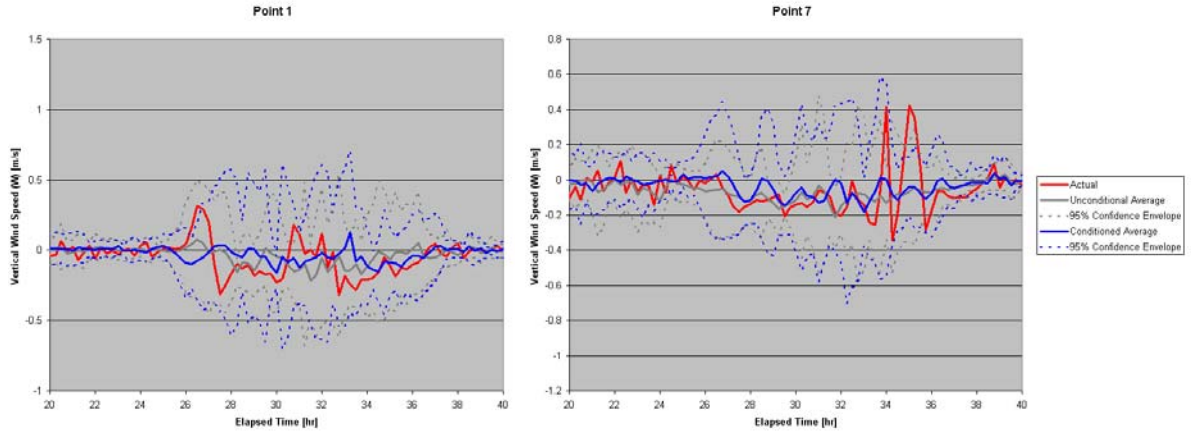

Figure 9: Conditioned average and actual vertical wind speed (W) at Point 1 and Point 7 during the recession period are shown with the conditioned 95% confidence interval. Unconditional average and envelope are also shown.

4.2 Conditional Simulations

Figures 7, 8 and 9 show the ensemble average saturation, latent heat flux and vertical wind speed, respectively, plotted with their 95 percent confidence envelopes and the actual values for each variable for the conditioned simulation. Also shown are the unconditional plots, for comparison. Using 320 conditioning points over the subsurface domain, there is a clear improvement in the 95 percent confidence envelope at Point 1 and Point 7 for both saturation and latent heat flux. The actual saturation at Point 1 remains at approximately 0.25 throughout the simulation. While the unconditioned 95 percent confidence interval ranging from 0 to 1 naturally includes the actual values, the conditioned envelope provides a meaningful estimate of the uncertainty. The ensemble averages for saturation and latent heat are in closer agreement with the actual values at both observation points in the conditioned case, compared with the unconditioned case, corresponding to nearly an order of magnitude decrease in root mean square error (RMSE) at Point 1, and a 50 percent decrease in RMSE at Point 7 for saturation. The decrease in RMSE for latent heat flux at Point 1 is approximately five-fold, and decreases by 0.8 W/m^2 at Point 7.

Ensemble averages for vertical wind speeds, as shown in Figure 9, appear to attenuate the sharp peaks that appear in the actual values for vertical winds for both the unconditional and the conditioned cases. It is possible that vertical winds may average to zero over a large number of realizations. If that is the case, then pointwise one-dimensional observations may not be appropriate for this analysis. A domain-averaged bulk approach may provide a more effective tool for analyzing the influence of conditioning in the heterogeneous subsurface on atmospheric processes.

5 CONCLUSIONS

- The rainfall area (Point 7) represents a highly controlled portion of the experiment. Variation in saturation between realizations is low in this area. Since latent heat flux is strongly correlated with saturation, its variation is also low in this area.
- Point 1, furthest from the rainfall, shows higher variation in saturation and latent heat flux. Conditioning of the subsurface heterogeneity in this area shows a larger effect on the 95 percent confidence envelope than at Point 7. The corresponding reduction in RMSE is larger at Point 1 when conditioning is applied.
- We can conclude that conditioning of the subsurface will have a strong influence on reducing uncertainties in variables that are directly related to subsurface properties, such as saturation and latent heat flux (as shown here), as well as runoff routing and evapotranspiration.
- It is less clear what influence subsurface conditioning has on atmospheric processes from the data analysis described here. Winds are a function of circulation across the entire domain and it is likely that the effect of conditioning does not manifest itself in a pointwise fashion as it does for saturation and latent heat flux. The variances in wind speeds that appear between realizations clearly indicate that the wind speeds are influenced by variation in the heterogeneous subsurface, since the subsurface is the only input variable that changes between realizations. As such it may be better to look at circulation in bulk over the entire domain. This could be accomplished using a

domain-averaged magnitude of the wind velocity instead of vertical wind speed at a point.

REFERENCES

[1] Tompson, A.F.B., R. Ababou, and L.W. Gelhar (1989). Implementation of of the three-dimensional turning bands random field generator. Water Resources Research, 25(10):2227–2243.

[2] Kollet, S. J., and R. M. Maxwell (2006). Integrated surface-groundwater flow modeling: A free surface overland flow boundary condition in a parallel groundwater flow model. Adv Water Resour, 29, 945-958.

[3] Skamarock, W.C., J.B. Klemp, J. Dudhia, D.O. Gill, D.M. Barker, M.G. Duda, X-Y. Huaang, W. Wang and J.G. Powers (2008). A Description of the Advanced Research WRF Version 3. NCAR Technical Note NCAR/TN-475+STR, 113p.

[4] Ashby, S. F., and R. D. Falgout (1996). A parallel multigrid preconditioned conjugate gradient algorithm for groundwater flow simulations. Nucl Sci Eng, 124, 145-159.

[5] Kollet, S.J. and R.M. Maxwell (2008). Capturing the influence of groundwater dynamics on land surface processes using an integrated, distributed watershed model, Water ResourcesResearch,44: W02402.

[6] Chen, F., and J. Dudhia, (2001a). Coupling an advanced land surface-hydrology model with the Penn State-NCAR MM5 modeling system. Part I: Model implementation and sensitivity. MonWeather Rev, 129, 569-585.

[7] Maxwell, R.M., J.K. Lundquist, J. Mirocha, S.G. Smith, C.S. Woodward, A.F.B. Tompson (2010 – in review). Development of a coupled groundwater-atmospheric model.